J|A|C|S ARTICLES

Published on Web 11/05/2009

Conjugated Polymers with Large Effective Stokes Shift: Benzobisdioxole-Based Poly(phenylene ethynylene)s

Tanmoy Dutta,[†] Kathy B. Woody,[†] Sean R. Parkin,[†] Mark D. Watson,*[,†] and Johannes Gierschner*[,‡]

Department of Chemistry, University of Kentucky, Lexington, Kentucky 40506-0055, and IMDEA Nanoscience, Madrid Institute for Advanced Studies, Madrid, Spain

Received August 21, 2009; E-mail: mdwatson@uky.edu; johannes.gierschner@imdea.org

Abstract: Phenyleneethynylene-based conjugated copolymers using benzo[1,2-d:4,5-d′]bis[1,3]dioxole (**BDO**) in the repeating unit are reported. The electronic structure of the **BDO** unit imparts a localized HOMO topology while the LUMO is delocalized over the polymer backbone, so that the lowest optical absorption band of the polymer has considerable intramolecular charge transfer character. This contrasts with published donor−acceptor polymers with localized LUMO and delocalized HOMO. The very large Stokes shifts of the monomers, which are due to the small oscillator strength of the lowest optical transition, are largely retained in the polymers as a result of covalently constrained dihedral angles in the substituents (not the backbone), as predicted/explained by calculations.

1. Introduction

Poly(phenylene ethynylene)s, PPEs, are conjugated polymers (CP)[1,2] that are studied as active components in organic (opto)electronic devices such as LEDs,[3] FETs,[4] and solar cells[5] and that have been commercialized in chemical and biological sensors.[6,7] The use of electron donor−acceptor architectures along the backbones of various CPs is a common tool to control morphological order and to tune optoelectronic properties.[8−13] Recently we reported PPE's built from alternating perfluorinated (acceptor) and peralkoxylated (donor) benzenes, as well as a transition-metal-free route for their synthesis exploiting fluoride ion catalyzed nucleophilic aromatic substitution.[14,15]

Surprisingly, the optical properties of these polymers built from highly oxygenated 1,2,4,5-tetraalkoxy benzenes (**TAB**) seemed fairly typical of PPEs. However, there were some slight differences between the different TAB-based polymers which were tentatively assigned to differing dihedral angles between the donor side chains and the polymer π-system, that is, mesomeric and inductive effects. As reported here, the electronic structure of the requisite 1,2,4,5-tetraalkoxy-3,6-diethynylbenzene monomers results in disjoint frontier molecular orbitals.[16,17] This imparts intramolecular charge transfer (ICT) character to the HOMO−LUMO optical transition and very large effective Stokes shifts (LSS) up to nearly 2 eV, which however does not persist in the corresponding PPEs built from these monomers. DFT calculations reported here explain this behavior and predict that if the α-carbons of the alkoxy side chains could be constrained close to the plane of the π-system, then the LSS can be maintained in polymers.

This constrained geometry is provided by benzo[1,2-d:4,5-d′]bis[1,3]dioxole (**BDO**) units. Based on the widely varying (opto)electronic properties of 3,4-dialkoxy- and 3,4-alkylenedioxythiophene polymers, one would expect significant differences in **BDO** and **TAB**-based CPs.[18] The electronic structure of **BDO** was exploited to study equilibria between electron- and charge-transfer states in donor−acceptor pairs and to measure the photoinduced charge separation distances in donor-spacer-acceptor systems.[19] **BDO** has also been used as the aryl unit in persistent trityl radicals for EPR imaging of biological

[†] University of Kentucky.
[‡] Madrid Institute for Advanced Studies.

(1) Bunz, U. H. F. *Chem. Rev.* **2000**, *100*, 1605–1644.
(2) Bunz, U. H. F. *Acc. Chem. Res.* **2001**, *34*, 998–1010.
(3) Voskerician, G.; Weder, C. *Adv. Polym. Sci.* **2005**, *177*, 209–248.
(4) Roy, V. A. L.; Zhi, Y.-G.; Xu, Z. -X.; Yu, S. -C.; Chan, P. W. H.; Che, C. -M. *Adv. Mater.* **2005**, *17*, 1258–1261.
(5) Mwaura, J. K.; Zhao, X.; Jiang, H.; Schanze, K. S.; Reynolds, J. R. *Chem. Mater.* **2006**, *18*, 6109–6111.
(6) Liao, J. H.; Swager, T. M. *Langmuir* **2007**, *23*, 112–115.
(7) Zheng, J. S.; Swager, T. M. *Adv. Polym. Sci.* **2005**, *177*, 151–179.
(8) Yamamoto, T.; Zhou, Z.-H.; Kanbara, T.; Shimura, M.; Kizu, K.; Maruyama, T.; Nakamura, Y.; Fukuda, T.; Lee, B.-L.; Ooba, N.; Tomaru, S.; Kurihara, T.; Kaino, T.; Kubota, K.; Sasaki, S. *J. Am. Chem. Soc.* **1996**, *118*, 10389–10399.
(9) Zhang, M.; Yang, C.; Mishra, A. K.; Pisula, W.; Zhou, G.; Schmaltz, B.; Baumgarten, M.; Muellen, K. *Chem. Commun.* **2007**, 1704–1706.
(10) Zhang, Q. T.; Tour, J. M. *J. Am. Chem. Soc.* **1998**, *120*, 5355–5362.
(11) Beaujuge, P. M.; Pisula, W.; Tsao, H. N.; Ellinger, S.; Muellen, K.; Reynolds, J. R. *J. Am. Chem. Soc.* **2009**, *131*, 7514–7515.
(12) Tsao, H. N.; Cho, D; Andreasen, J. W.; Rouhanipour, A.; Breiby, D. W.; Pisula, W.; Muellen, K. *Adv. Mater.* **2009**, *21*, 209–212.
(13) van Mullekom, H. A. M.; Vekemans, J. A. J. M.; Havinga, E. E.; Meijer, E. W. *Mater. Sci Eng., R* **2001**, *32*, 1–40.
(14) Dutta, T.; Woody, K. B.; Watson, M. D. *J. Am. Chem. Soc.* **2008**, *130*, 452–453.
(15) Woody, K. B.; Bullock, J. E.; Parkin, S. R.; Watson, M. D. *Macromolecules* **2007**, *40*, 4470–4473.
(16) Zucchero, A. J.; Wilson, J. N.; Bunz, U. H. F. *J. Am. Chem. Soc.* **2006**, *128*, 11872–11881.
(17) Fahrni, C. J.; Yang, L.; VanDerveer, D. G. *J. Am. Chem. Soc.* **2003**, *125*, 3799–3812.
(18) Groenendaal, L.; Zotti, G.; Aubert, P. H.; Waybright, S. M.; Reynolds, J. R. *Adv. Mater.* **2003**, *15*, 855–879.
(19) (a) Sun, D.; Rosokha, S. V.; Kochi, J. K. *J. Phys. Chem. B.* **2007**, *111*, 6655–6666. (b) Carmieli, R.; Mi, Q.; Ricks, A. B.; Giacobbe, E. M.; Mickley, S. M.; Wasielewski, M. R. *J. Am. Chem. Soc.* **2009**, *131*, 8372–8373.

systems.[20] Interestingly, fusion of dioxole rings to the terminal positions of acenes, in the place of alkoxy chains, made relatively little difference in the optoelectronic properties.[21] However, donor−acceptor dyads with C60 bismethano-fullerenes as acceptor showed significantly different photoinduced charge transfer behavior depending on whether the donor was a **TAB** or **BDO**.[22]

In this work we have introduced **BDO** into the conjugated backbones of two poly(phenylene ethynylene)s (PPE) and a poly(phenylene diethynylene) (PEE) resulting in polymers with localized HOMO and delocalized LUMO, opposite to fairly commonly observed localized LUMO and delocalized HOMO in D−A polymers. For example, our calculations (not shown) confirm the latter case for the benzothiadiazole-containing PPE of Bunz[23] and the cyclopentadienone-containing polythiophene of Wudl.[24] Unlike here, LSS in conjugated polymers is typically attributed to large conformational differences between the ground and excited states. The very large effective Stokes shifts (LSS) demonstrated by the **BDO** polymers (0.7 to 0.9 eV), may be useful to minimize self-absorption and light scattering in optical materials.[25] Possible applications include laser dyes, molecular imaging, scintillators, solar collectors and white light emitting materials.[26−29] In a quantum-chemical approach using density-functional theory we fully elucidate the reasons for the electronic and optical properties of the new **BDO**-based polymers and compare them to the analogous **TAB** PPEs.

2. Experimental Section

Characterization. Solution photoluminescence (10^{-8} M THF) and UV−vis absorption spectra (10^{-6} M THF) were measured on a Fluorolog-3 fluorometer and Varian CARY 1 spectrophotometer. Solid state spectra were recorded from thin films spin-coated from solution (∼0.5 mg/mL toluene) onto quartz plates.

Electrochemical measurements were performed under nitrogen atmosphere using a BAS-CV-50W voltametric analyzer and three electrode cell (platinum working, silver wire counter and pseudoreference electrodes). The supporting electrolyte solution (0.1 M $(n\text{-Bu})_4NPF_6$, anhydrous CH_3CN) was thoroughly purged with nitrogen before each measurement, and ferrocene/ferrocenium (Fc/Fc^+, $E_{1/2} = 0.46$ V) was used as reference. Polymers were evaluated as thin films solvent cast directly onto the working electrode while small molecules were evaluated in dilute CH_3CN solution. Detailed procedures for monomer and polymer syntheses and their characterization are included in the Supporting Information. Monomer **M3** and polymer **TABFPPE** (Table 1, R = 3,7-dimethyloctyl) were prepared as published.[14]

Theoretical Methodology. The geometry and electronic structure of the molecules were calculated at the density functional theory (DFT) level using the B3LYP functional and the 6-311G* basis set. Comparative calculations showed that the dioxole ring is slightly nonplanar in agreement with experiment,[30] thus no symmetry restrictions were imposed. Vertical optical transition energies and oscillator strengths were obtained by time-dependent (TD)DFT. All calculations were carried out within the Gaussian03 program package.[31] Orbital pictures were produced with Molekel 4.3.[32]

3. Results

Synthesis. An alkylated benzo[1,2-d:4,5-d′]bis[1,3]dioxole (BDO, **3**, Scheme 1) was synthesized by modified published procedures in good yield.[20] BDO **3** was intentionally prepared as a complex mixture of stereoisomers to enhance solubility of the resulting polymers. R and R′ may be syn or anti about the benzene ring plane and the 2-ethylhexyl chains are derived from a racemic starting material. Our first PPEs based on highly symmetric or slightly lower symmetry **BDO**s carrying linear side chains (e.g., **BDOFPPE**, scheme 2, R = R′ = *n*-hexyl; or R = *n*-hexyl, R′ = ethyl, not shown) were soluble in common organic solvents only at elevated temperature. Lithiation of **3** with BuLi/TMEDA and quenching with I_2 produced the diodo BDO **4**, from which monomer **M1** was synthesized by Pd-catalyzed Negishi coupling.

Polymer **BDOFPPE** was prepared via nucleophilic aromatic substitution,[14] with the fluoride-activated silyl-acetylene groups of monomer **M1** acting as nucleophiles and hexafluorobenzene acting as electrophile (Scheme 2). Multinuclear NMR spectra (^{19}F, ^{1}H, ^{13}C, Supporting Information) indicate high structural purity for **BDOFPPE**, similar to previously reported **TAB**-based PPEs. Polymers **BDOPPE** and **BDOPEE** were synthesized using Pd-catalyzed cross- and homocoupling polymerizations, respectively.

Optical Properties. The solution UV/vis absorption spectra (Figure 1a,b) of the polymers **TABFPPE**, **BDOPEE**, **BDOPPE** and **BDOFPPE** exhibit similar features, dominated by a strong absorption maximum (A_{max}) around 400 nm, similar to many other PPEs.[1,2] Also similar to most PPEs, the separation between A_{max} and the photoluminescence maximum (PL_{max}), or Stokes shift, is relatively small for **TABFPPE** (0.15 eV). The absorbance spectra of the three **BDO**-based polymers, however, contain a more or less pronounced shoulder (A_1, Figure 1a, b) at the low energy side of A_{max}. This is intrinsic to the diluted polymers (i.e., contamination and aggregation as a possible source for A_1 were excluded), and is thus assigned to the ground to first excited state transition ($S_0 \rightarrow S_1$). The PL spectra of the **BDO**-based polymers are strongly red-shifted against the main absorption band (Figure 1a). This gives large effective Stokes shifts, varying between 0.75 and 0.95 eV (Table 1) and larger than those reported for most conjugated polymers so far.[26,27,33] The Stokes shifts for the monomers **M1**, **M2**, and **M3** are even larger at 1.45, 1.89, and 1.12 eV, respectively. While the LSS for **M1** and **M2** are mainly due the large separation between A_{max} and A_1, (1.14 and 1.55 eV), the shift for **M3** is mainly due to the large distance between A_1 and PL_{max} (0.72 eV), see Table 1. The latter is attributed to the larger steric effects of

(20) Reddy, T. J.; Iwama, T.; Halpern, H. J.; Rawal, V. H. *J. Org. Chem.* **2002**, *67*, 4635–4639.
(21) Anthony, J. E.; Gierschner, J.; Landis, C. A.; Parkin, S. R.; Sherman, J. B.; Bakus, R. C., II *Chem. Commun.* **2007**, *45*, 4746–4748.
(22) Zheng, J.-Y.; Noguchi, S.; Miyauchi, K.; Hamada, M.; Kinbara, K.; Saigo, K. *Fullerene Sci. Techn.* **2001**, *9*, 467–475.
(23) Bangcuyo, C. G.; Evans, U.; Myrick, M. L.; Bunz, U. H. F. *Macromolecules* **2001**, *34*, 7592–7594.
(24) Walker, W.; Veldman, B.; Ciechi, R.; Patil, S.; Bendikov, M.; Wudl, F. *Macromolecules* **2008**, *41*, 7278–7280.
(25) Vollmer, F.; Rettig, W.; Birckner, E. *J. Fluoresc.* **1994**, *4*, 65–69.
(26) Liu, K.; Li, Y.; Yang, M. *J. Appl. Polym. Sci.* **2009**, *111*, 1976–1984.
(27) Rabindranath, A. R.; Zhu, Y.; Heim, I.; Tieke, B. *Macromolecules* **2006**, *39*, 8250–8256.
(28) Yang, C.; Jacob, J.; Muellen, K. *Macromolecules* **2006**, *39*, 5696–5704.
(29) Kim, Y.; Whitten, J. E.; Swager, T. M. *J. Am. Chem. Soc.* **2005**, *127*, 12122–12130.
(30) Laane, J.; Bondoc, E.; Sakurai, S.; Morris, K.; Meinander, N. *J. Am. Chem. Soc.* **2000**, *122*, 2628–2634.
(31) Frisch, M. J.; et al. *GAUSSIAN 03*, revision C.02; Gaussian, Inc., Wallingford, CT 2004.
(32) Flukiger, P.; Portmann, H. P. L., S.; and Weber, J. *MOLEKEL: An Interactive Molecular Graphics Tool*; Swiss Center for Scientific Computing: Manno, Switzerland, 2000−2002.
(33) Egbe, D. A. M.; Ulbricht, C.; Orgis, T.; Carbonnier, B.; Kietzke, T.; Peip, M.; Metzner, M.; Gericke, M.; Birckner, E.; Pakula, T.; Neher, D.; Grummt, U.-W. *Chem. Mater.* **2005**, *17*, 6022–6032.

Table 1. Experimental Transition Energies of the Monomers and Polymers, from Solution Measurements (**BDO** Side Chains Omitted for Clarity)

	Backbone structure	$E(A_1)$ [a] eV [nm]	$E(A_{max})$ [b] eV [nm]	$\Delta E(A_{max}\text{-}A_1)$ [c] eV	f_1/f_{max} [d]	$E(PL_{max})$ [e] eV [nm]	ΔE_{Stokes} [f] eV	ΔE_{AE} [g] eV
M1	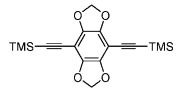	3.04 [408]	4.18 [297]	1.14	0.10	2.73 [455]	1.45	0.31
M2		3.13 [396]	4.68 [265]	1.55	0.43	2.79 [444]	1.89	0.34
M3	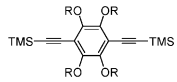	3.73 [333]	4.13 [300]	0.4	0.10	3.01 [412]	1.12	0.72
BDOPEE	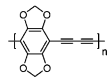	2.69 [461]	3.04 [407]	0.35	0.17	2.28 [544]	0.76	0.39
BDOPPE	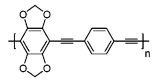	2.96 [419]	3.21 [386]	0.25	0.18	2.40 [517]	0.81	0.56
BDOFPPE	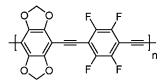	2.70 [459]	3.07 [404]	0.35	0.11	2.12 [585]	0.95	0.58
TABFPPE	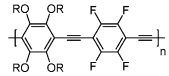	--	2.96 [419]	--	--	2.81 [442]	0.15	--

[a] Energies of absorption preband. [b] Energies of absorption maximum. [c] Energy separation. [d] Ratio of oscillator strengths. [e] PL maximum. [f] Stokes shift $\Delta E_{Stokes} = E(A_{max}) - E(PL_{max})$. [g] Energy separation $\Delta E_{AE} = E(A_1) - E(PL_{max})$. For polymers, the position of the A_1 state was extracted from a Gaussian fit to the filled part of the spectrum (Figure 1a), where the same half-width was applied for all polymers.

the alkoxy chains in **M3** compared to **M1**, and stronger Franck−Condon activity of torsional modes. A clear correlation of the PL_{max} energy with the A_1 position is observed for the polymers, yielding an energy spacing of 0.4−0.6 eV (Table 1), as might be expected since PL should originate from S_1. The polymers show a distinct solvatochromism of the PL spectra, as exemplified for **BDOFPPE** in Figure 2. With increasing solvent polarity, the emission is shifted to longer wavelength and PL intensity decreases, suggesting intramolecular charge-transfer (ICT) contributions to the emitting state. In the solid state, the optical properties are essentially preserved (Supporting Information). The absorption and emission spectra are red-shifted by ca. 0.05 eV against solution and the effective Stokes shift is of the same magnitude as in solution. The colors of the solid polymers range from yellow for **BDOPEE** and **BDOPPE** to red-orange for **BDOFPPE**. The last is quite different from PPEs based on dialkoxybenzenes[1,2] and the more structurally similar **TABFPPE** (Figure 1a), which rather emit in the blue-green.

4. Discussion

The electronic differences between **BDO**s and **TAB**s become clear during the synthesis of the monomers. Bislithiation at the 3,6-positions of **BDO**s (step "v", Scheme 1) requires more forcing conditions (TMEDA, *n*-BuLi) compared to **TAB**s (*n*-BuLi, hexanes). This may be a combination of the differing abilities of the **TAB** or **BDO** ether oxygens to coordinate to lithium cations, the differing inductive and mesomeric effects of the pendant oxygen atoms, and deviation in hydridization, from sp^2 toward sp^3, of the carbons to be deprotonated. The C−C−C bond angles around the protonated benzene carbons of **BDO** are 115.5° (cif file, Supporting Information) compared to the approximately 120° angles of **TAB**s.[34] This is also reflected in the differences in the ^{1}H NMR chemical shifts of the phenyl protons, that is, 6.2 ppm for **BDO** (**3**) versus 6.5−6.6 ppm for **TAB**s.

Monomer **M1** is isolated as a complex mixture of stereoisomers. Thin layer chromatography of other asymmetric **BDO**s, namely bearing ethyl and hexyl chains (not shown) indicated that *syn*- and *anti*-isomers can be separated. This additional structural variability provides another means to engineer solubility and thermal properties of the polymers. A single stereoisomer crystallizes from the oily mixture of **M1** stereoisomers on storage at low temperature, and its crystallographic information file can be found in the Supporting Information. The **BDO** ring system is essentially flat, with acetal carbons deviating just 0.17 Å from the plane of the benzene ring, in contrast to **TAB**s,[34] where the *O*-α-carbon bonds of the side chains are nearly

(34) Keegstra, E. M. D.; Huisman, B.-H.; Paardekooper, E. M.; Hoogsteger, F. J.; Zwikker, J. W.; Jenneskens, L. W.; Kooijman, H.; Schouten, A.; Veldman, N.; Spek, A. *J. Chem. Soc., Perkin Trans. 2* **1996**, *2*, 229–240.

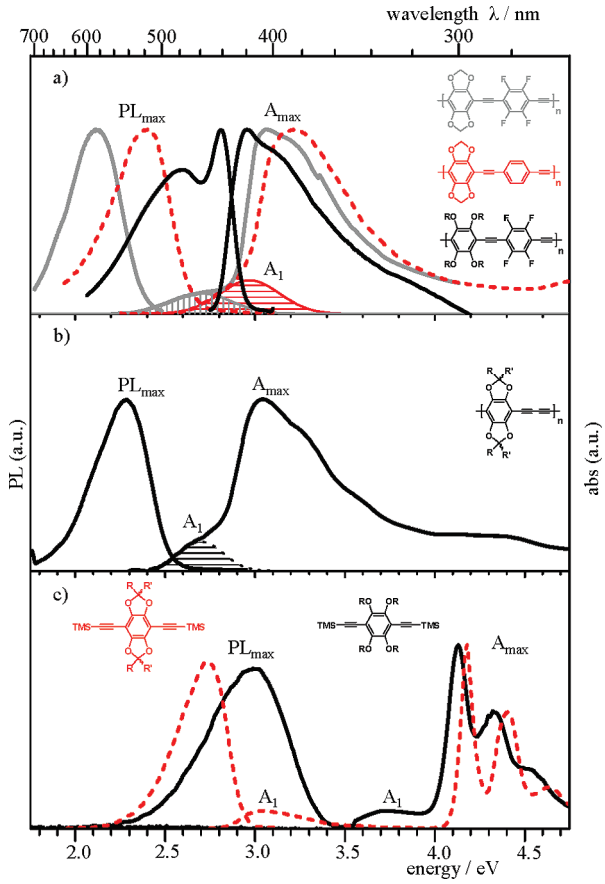

Figure 1. PL (10^{-8} M THF) and UV/vis absorption spectra (10^{-6} M THF). Filled areas are the deconvoluted A_1 states (see text). **BDO** side chains omitted for clarity. All spectra normalized.

Scheme 1. Monomer Synthesis[a]

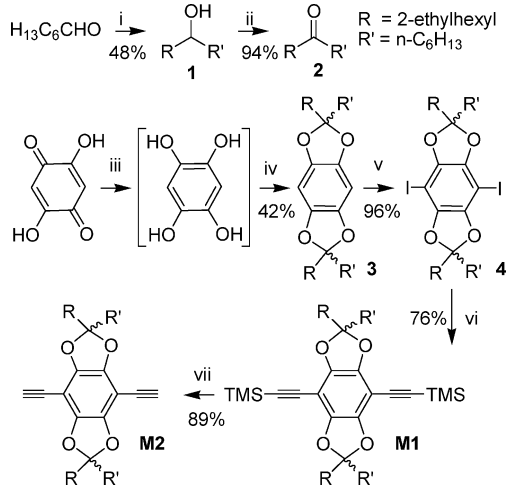

[a] (i) 2-Ethylhexyl magnesium bromide; (ii) PCC-alumina, hexanes, 60°C; (iii) H_2, Pd/C, THF; (iv) PPTS, toluene, **2**, reflux; (v) (1) BuLi, hexanes, TMEDA (2) I_2; (vi) ClZnCCTMS, Cl_2Pd[dppf], THF; (vii) KOH, EtOH.

perpendicular to the benzene plane. In addition to ring-strain effects, this difference must significantly change the mesomeric/inductive influence of the substituents, imparting the (opto)-electronic properties of the **BDO** monomers and polymers.

To elucidate the nature of the absorbing and emitting states, quantum-chemical calculations were carried out on the corresponding oligomers and polymer properties were obtained by

Scheme 2. Polymer Synthesis[a]

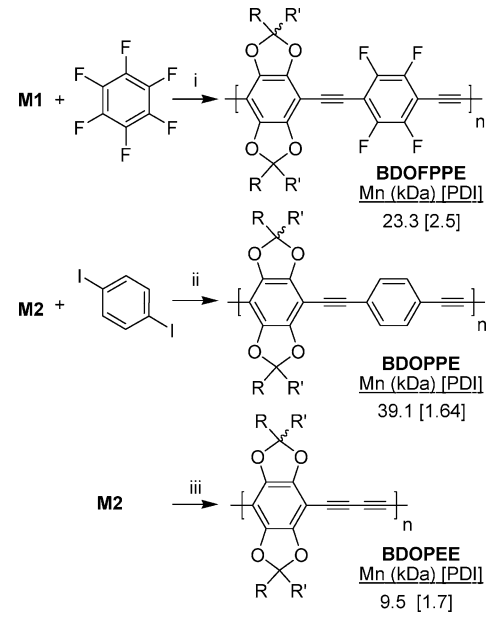

[a] (i) TBAF, toluene; (ii) $Pd(PPh_3)_4$, CuI, toluene, DIPA, 60°C; (iii) $Pd(PPh_3)_4$, CuI, benzoquinone, toluene, DIPA, 60 °C.

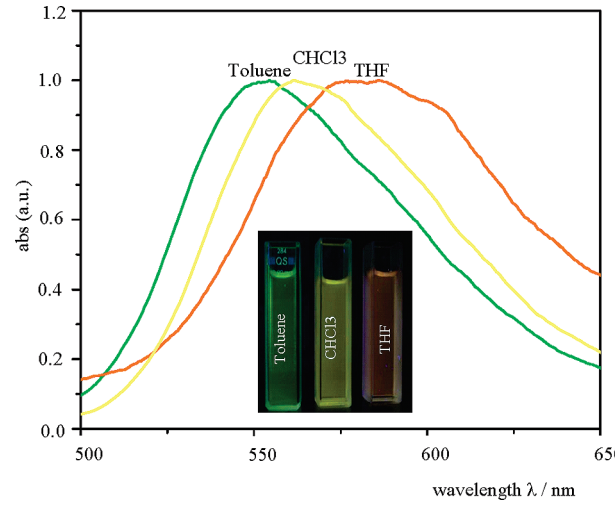

Figure 2. PL solvochromism of **BDOFPPE** (10^{-8} M). All spectra normalized. (Inset) Optical photograph of solutions under 365 nm irradiation.

an extrapolation procedure.[35] For consistency in comparing unsubstituted parent homopolymer **PPE** to the newly reported alternating copolymers having the same size π-system, a variable length "*n*" was defined as the number of alkyne linkages within a series of oligomers. The number of benzene units then equals $n + 1$. For example, the **PPE** and **BDOFPPE** structures in Figure 3 both correspond to $n = 3$, despite their differing numbers of constitutional repeating units.

In *unsubstituted* oligomers and polymers of the **PPE** type and others including poly(phenylene vinylene) or poly(thiophene), the first excited state (S_1) is usually optically strongly allowed, as indicated by the calculated oscillator strengths (*f*) for **PPE** (Table 2). In these classes of materials, the S_1 state is mainly composed of the HOMO to LUMO (H→L)

(35) Gierschner, J.; Cornil, J.; Egelhaaf, H.-J. *Adv. Mater.* **2007**, *19*, 173–191.

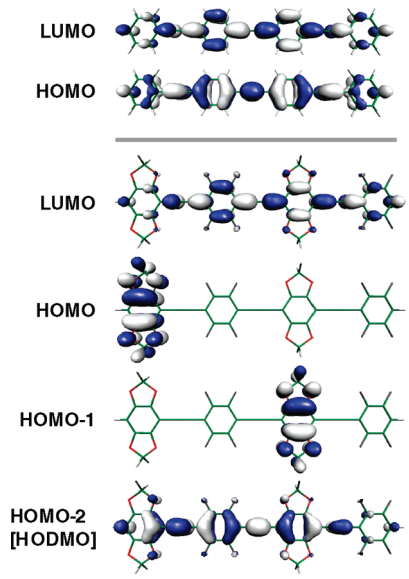

Figure 3. Frontier orbital topologies (DFT) for oligomers ($n = 3$) of **PPE** (top) and **BDOFPPE** (bottom).

transition, where both H and L are delocalized along the polymer backbone. This is illustrated in the orbital pictures for an oligomer of the parent **PPE** at the top of Figure 3. This also accounts for the optical characteristics of most of the substituted species studied so far.

For **BDOFPPE** oligomers, the situation is very different. The S_1 state is still mainly composed from the H → L transition, but is only weakly allowed, as seen from the TD-DFT calculated oscillator strengths (f, Table 2). This is due to the very different topology of the HOMO orbital, which is here entirely localized in the **BDO** unit, whereas the LUMO is delocalized along the backbone (Figure 3, bottom), thus imparting pronounced ICT character to S_1. The first strongly allowed transition, which gives rise to A_{max} (Figure 1a), is a higher S_x state ($x = (n + 3)/2$) mainly composed of H-x-1 → L, with n being the number of alkyne linkages as defined above (Table 2). The H-x-1 orbital for each oligomer is delocalized along the backbone and therefore is the highest occupied delocalized molecular orbital (HODMO). The S_x state corresponds to the S_1 state in unsubstituted **PPE** and is very similar in energy.

The localized nature of the HOMO orbital can be rationalized by a simple exercise in combining the frontier orbitals of subunits, e.g. **BDO** and a fluorinated phenyleneethynylene (**FPE**) (Figure 4). The LUMOs of **BDO** and **FPE** are relatively close in energy, combining to give delocalized MOs (L, L+2). On the other hand, the energy separation of the HOMOs of the subunits is large, $\Delta E = 2.03$ eV. Thus, the original HOMOs of both **BDO** and **FPE** remain localized, whereas the H-1 of **BDO** interacts with the energetically close H-1 of **FPE** forming a delocalized MO (H-1). Note that a cross-combination of H of one unit with H-1 of the other unit is not possible due to symmetry mismatch. It is thus the unusually high-lying HOMO of **BDO** which leads to the localized HOMO topology in the oligomers and polymers.

Calculations show that with increasing chain length n, the energy spacing $\Delta E(S_x - S_1)$ and thus $\Delta E(A_{max} - A_1)$ becomes smaller (Table 2 and Figure 5) in agreement with experiment. For example, the experimentally measured $\Delta E(A_{max} - A_1)$ values are approximately 1.55 eV for monomer **M2**, but only 0.35 eV for the corresponding polymer **BDOFPPE** (Figure 1b). The decrease of $\Delta E(S_x - S_1)$ with n is readily seen from the energetic positions of the frontier orbitals plotted in Figure 5. The energy of the delocalized LUMO decreases, while the HODMO energy increases with n due to the extension of the conjugated π-system, leading to a steep decrease of $E(S_x)$ with n. On the other hand, the localized HOMO remains almost unchanged in energy, thus yielding a smaller decrease of $E(S_1)$ compared to $E(S_x)$ with increasing chain length.

Extrapolating to the polymer limit, the calculation yields an energetic separation between A_1 and A_{max}, of ca. 0.2 eV, not far away from experiment $\Delta E(S_x - S_1) = 0.35$ eV (Table 1). The deviation is ascribed to the shortcomings of the used B3LYP functional, which is known to overestimate the chain length dependence of transitions between delocalized orbitals,[35] in our case between HODMO and LUMO, whereas the HOMO−LUMO transition is less affected due to the localized HOMO.

How important is fluorine for the ordering of the states? To answer this question, calculations were also carried out on a series of nonfluorinated **BDOPPE** oligomers. Within this series the HOMO is again localized, while the LUMO is delocalized. The energy difference between the HOMO and the HODMO again decreases with n, and to a much smaller value, for example, 0.03 eV for $n = 7$ compared to 0.36 eV for the fluorinated **BDOFPPE**[36] (Figure 5). The difference between the two systems results from the high electronegativity of fluorine, which generally stabilizes the orbitals.[37] However, this is only valid for orbitals with a significant contribution from the fluorine-substituted rings, thus in particular for the delocalized orbitals (LUMO, HODMO), see Figure 3. The energy of the HOMO, which is localized on the **BDO** unit, decreases only slightly with fluorination of neighboring rings. Thus, the energy difference between HOMO and HODMO and thus $\Delta E(S_x - S_1)$ will be larger in the fluorinated compounds, in agreement with the experimental findings, see Table 1. The virtual independence of HOMO energy on whether or not fluorine is present agrees with the electrochemical measurements of **BDOPPE** and **BDOFPPE** (Table 3). The oxidation potentials for both polymers agree to within 0.01 V (0.01 eV difference in E_{HOMO}), within experimental error.

How important is the **BDO** unit for the ordering for the states? Upon replacing **BDO** by **TAB** in an oligomer with $n = 1$, the localized HOMO is stabilized by −0.2 eV, whereas the HODMO is destabilized by 0.2 eV, see Figure 5. Thus, an ICT emitting state is predicted for short oligomers, in agreement with a large experimental effective Stokes shift and absorbance preband for **TAB**-based monomer **M3** (Figure 1c). On the other hand, for longer chain length n an early crossing of the HOMO with the HODMO is expected (Figure 5). At the polymer limit the lowest excited state will be determined by the HODMO-LUMO transition typical for PPEs, and no low intensity ICT preband or large Stokes shift is expected, in agreement with the experimental results for the polymer **TABFPPE** in solution (Figure 1a).[14] It is important to note that the MO energies critically depend on the geometry of the **TAB** units. The calculations described above employed the lowest energy side-chain conformation, with the sp^3 α-carbons of the ether chains

(36) For the electronic states in **BDOPPE**s, this leads to a crossing of the ICT state with the delocalized state, thus (TD-)DFT predicts ICT not to be the lowest state in **BDOPP**E in contradiction with experiment, which is again due to the shortcomings of (TD-)DFT for polymers, vide infra.

(37) Milián Medina, B.; Beljonne, D.; Egelhaaf, H.-J.; Gierschner, J. *J. Chem. Phys.* **2007**, *126*, 111101.

Table 2. Calculated Electronic Levels (E_{HOMO}, E_{LUMO}), Band Gap $\Delta E_{H\text{-}L}$, Vertical Transition Energies E_{vert} and their Composition (Configuration Interaction, or "CI" Contributions) and Oscillator Strengths *f* of the First Two Optical Transitions S_1, S_2

		DFT				TD-DFT			
polymer	n^a	$E_{HODMO}{}^b$ (eV)	E_{HOMO} (eV)	E_{LUMO} (eV)	$\Delta E_{H\text{-}L}$ (eV)	E_{vert}	main CI contrib.	*f*	ΔE (S_1-S_2)
PPE	1		−5.963	−1.530	4.43	S_1: 4.16	H→L	0.94	
	3		−5.603	−2.236	3.37	S_1: 3.07	H→L	2.73	
	7		−5.491	−2.533	2.96	S_1: 2.60	H→L	5.66	
BDOPPE	1	−5.913 [H-1]	−5.333	−1.539	3.79	S_1: 3.34	H→L	0.06	0.73
						S_2: 4.07	H-1→ L	0.93	
	3	−5.542 [H-2]	−5.373	−2.191	3.18	S_1: 2.85	H→L	0.03	0.19
						S_2: 2.85	H-1→L	0.04	
						S_3: 3.04	H-2→ L	2.71	
	5	−5.452 [H-2]	−5.381	−2.375	3.01	S_1: 2.73	H-2→L	4.12	
						S_2: 2.73	H-3→L	0.10	
						S_3: 2.75	H-1→L	0.03	
						S_4: 2.75	H→L	0.01	
	7	−5.417 [H-1]	−5.383	−2.542	2.84				
BDOFPPE	1	−6.353 [H-1]	−5.500	−2.071	3.43	S_1: 2.99	H→L	0.04	0.99
						S_2: 3.98	H-1→L	0.90	
	3	−5.993 [H-2]	−5.497	−2.704	3.08	S_1: 2.47	H→L	0.01	0.51
						S_2: 2.57	H-1→L	0.04	
						S_3: 2.98	H-2 → L	2.66	
	5	−5.909 [H-3]	−5.515	−2.892	2.62	S_1: 2.39	H→L	0.01	0.28
						S_2: 2.43	H-1→L	0.03	
						S_3: 2.47	H-2→L	0.03	
						S_4: 2.67	H-3→L	4.10	
	7	−5.876 [H-4]	−5.515	−2.969	2.54				

[a] *n* = number of alkyne linkages. The number of benzene rings = n + 1. See for example the structures in Figure 3 where *n* = 3. [b] HODMO = Highest occupied *delocalized* molecular orbital.

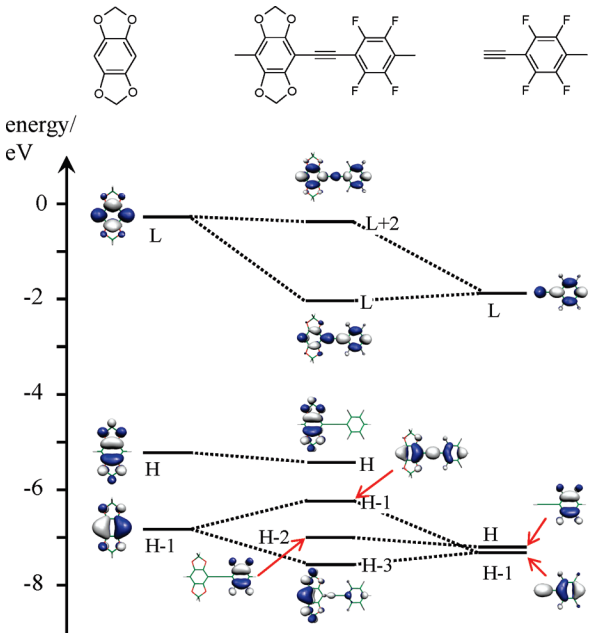

Figure 4. Correlation diagram for the frontier molecular orbitals of a single **BDOFPPE** linkage from the corresponding subunits at the DFT B3LYP/6-311G* level of theory.

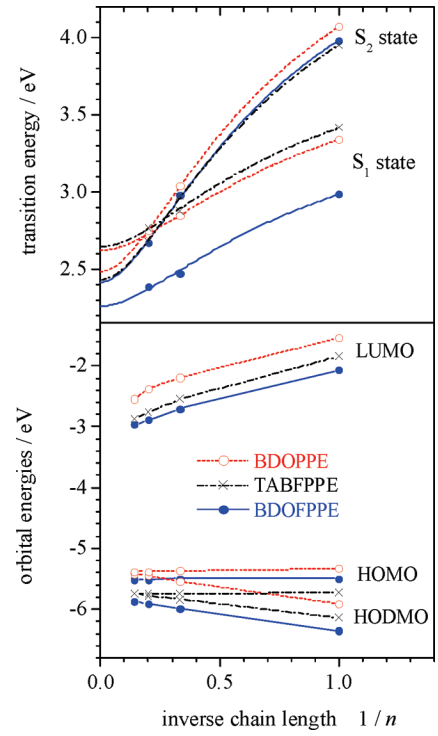

Figure 5. (TD-)DFT calculated electronic transition energies (top) and orbital energies (bottom) of **BDOPPE** (○), **BDOFPPE** (●) and **TABFPPE** (×) as a function of the inverse chain length 1/*n*, where *n* = number of alkyne linkages.

extending out of the plane of the benzene ring. For an imposed all-planar (or nearly planar) structure, the calculated MO energies and thus optical transitions are more similar to **BDO**-based polymers.

The localized topology of the HOMO orbital of the novel copolymers is thus a very peculiar electronic feature imposed by the **BDO** unit, which is not only found for short oligomers as in the **TAB** case, but also at the polymer limit. HOMO localization is typically not known in common all-conjugated donor−acceptor (D−A) type copolymers. For conventional materials built from units with pronounced ICT character,[38] the ICT character becomes typically smaller with increasing chain

Table 3. Electrochemical Data (eV)

	E_g^{opt} [a]	$E_{1/2}$ [b]	E_{HOMO} [c]	E_{LUMO} [d]	$E_{HOMOcalc}$
3	3.6	0.32	−5.1	−1.5	−5.24[e]
M1	3.0	0.57	−5.4	−2.4	NA
M2	3.0	0.56	−5.4	−2.4	−5.49[e]
BDOFPPE	2.4	0.81	−5.6	−3.2	−5.52[f]
BDOPPE	2.7	0.68	−5.5	−2.8	−5.38[f]
BDOPEE	2.6	0.80	−5.6	−3.0	−5.47[f]

[a] Optical energy gap from intersection of absorption and emission in solution. [b] Half-wave oxidation potential referenced to Fc/Fc^+ couple (0.46 V). [c] $E_{HOMO} = -(E^{1/2}_{ox} + 4.8)$ eV. [d] Calculated at a first approximation from $E_{LUMO} = E_{HOMO} + E_g^{opt}$. [e] DFT calculations. [f] Extrapolation of the DFT values in Table 2 to the polymer limit.

length,[39] thus preserving only a partial ICT character of the frontier orbitals at the polymer limit.[39−41] Moreover, in D−A polymers reported so far, the LUMO is generally more localized than the HOMO[38,39,41] opposite to the polymers studied here. This is due to typically larger differences in the LUMO energies, compared to the HOMO energies, of the donor and acceptor building blocks.[38] A PPE copolymer reported by Swager,[42] composed of alternating pentiptycene and diaminobenzene units, also yields a large energy spacing between absorption and PL maxima, however with an absorption preband of much higher absorbance than in the polymers reported by us. Given the very bulky nature of the repeating units, the energy shift was reasonably attributed to large conformational differences between ground and excited states. Preliminary calculations by us (not shown) support this geometrical concept, but also stress the contribution of localized occupied frontier orbitals at the pentiptycene units in a rather complex CI description of the lowest excited state. This indicates that the right choice of the D and A building blocks for the polymer repeating units—which can be conveniently assisted by appropriate quantum-chemical methods—opens the pathway to design polymers with precisely defined orbital energies and topologies, and thus to tailor the electronic and optical properties, which govern the electron and energy transport in the active organic layer of opto-electronic devices.

5. Conclusion

We have synthesized and characterized new conjugated copolymers based on a benzodioxole (**BDO**) and phenylene-ethynylene (PE) repeating units. Very different to donor−acceptor copolymers reported so far, the new copolymers display a peculiar electronic structure with localized HOMO and delocalized LUMO topologies. The HOMO localization is due to the high lying HOMO of the constituent **BDO** unit, which cannot mix with the respective MO of the PE unit. As a consequence, the lowest optical transition shows a pronounced ICT character and shows up as a low-intensity preband below the intense main absorption band. The latter is composed from delocalized orbitals as in common conjugated polymers. Very large effective Stokes shifts of these materials both in solution and the solid state are thus observed, extending those of polymers reported in literature. Future derivatives might thus be good candidates for large Stokes shift applications, e.g. lasers, molecular imaging, scintillators, solar collectors and white light emitting materials. Further, bulky substituents which will be orthogonal to the polymer backbones when attached to the **BDO** acetal carbons, should lead to intrinsically nanoporous polymers as hosts/sensors for electron-accepting guests/analytes.

Acknowledgment. M.D.W. and T.D. thank the National Science Foundation (CHE 0616759) for financial support. J.G. is a "Ramón y Cajal" research fellow, financed by the Spanish Ministry for Science and Innovation (MICINN). At the present, he is a visiting researcher at the ICMol, University of Valencia, in the framework of the MICINN Consolider Ingenio 2010 Molecular Nanoscience program.

Supporting Information Available: Experimental procedures, spectroscopic, electrochemical and crystallographic data. Complete refs 31 and 39. This material is available free of charge via the Internet at http://pubs.acs.org.

JA9068134

(38) Cornil, J.; Gueli, I.; Dkhissi, A.; Sancho-Garcia, J. C.; Hennebicq, E.; Calbert, J. P.; Lemaur, V.; Beljonne, D.; Brédas, J. L. *J. Chem. Phys.* **2003**, *118*, 6615.
(39) Reynolds, J. R.; et al. *J. Am. Chem. Soc.* **2009**, *131*, 2824–2826.
(40) Herbert, M. *Angew. Chem., Int. Ed.* **2005**, *44*, 2482–2506.
(41) Karsten, B. P.; Bijleveld, J. C.; Viani, L.; Cornil, J.; Gierschner, J.; Janssen, R. A. J. *J. Mater. Chem.* **2009**, *19*, 5343–5350.
(42) Thomas III, S. W.; Swager, T. M. *Macromolecules* **2005**, *38*, 2716–2721.